Response to Referee #2

Dear Editor and Dr. Jonas Elm,

We thank you very much for the professional and careful review of our manuscript "***Altitude-Dependent Role of Nitric Acid in Iodic Acid-Iodous Acid Nucleation: From Marine Boundary Layer Catalyst to Upper Troposphere Core Component***" (MS No.: egusphere-2026-1771). Accordingly, we have revised the manuscript and the Supporting Information. Our point-by-point responses to Dr. Jonas Elm's comments are given below.

Referee's recommendation: Zhang et al. investigates the effect of nitric acid (HNO_3) on the clustering of iodic acid (HIO_3) and iodous acid (HIO_2). The $(HIO_3)_n(HIO_2)_m$ cluster structures are taken from previous work by the same group, and the current investigation feels like a natural extension.

The cluster configurations are sampled using well-established protocols and state-of-the-art quantum chemical methods. The calculated thermochemistry is used in the atmospheric cluster dynamics code (ACDC) to simulate new particle formation (NPF) rates. Specifically, the authors simulate NPF at Zhejiang, Mace Head, Greenland and in the upper troposphere. The overall finding is that HNO_3 contributes to cluster formation in all regions. I find the altitude analysis performed in this manuscript particularly interesting and extremely well carried out. This is good inspiration for other work in the field.

I only have minor issues with the justification of the applied methods. I.e. how much can we trust that the methods are giving reliable results, without backing up the accuracy of the methods. I acknowledge that the sensitivity tests alleviate some of this concern, but it does not give the full picture.

Overall, the paper is interesting, well-written and advances our understanding of NPF in the marine environment. I believe it is a good fit for ACP and recommend publication after the following comments have been addressed.

Response: We sincerely appreciate Dr. Jonas Elm's positive feedback on our work. We highly value your constructive comments concerning the reliability and accuracy of our methods. Corresponding revisions have been made to the manuscript as suggested.

Comment 1 (Line 72). *"… with detailed procedures provided in the Supporting Information"*

I would appreciate that the sampling details are also included in the methods. Hence, integrate the "Multi-step cluster conformational search method" from the SI to the methods section as this will make it more transparent whether one can trust the found structures.

In addition, the applied UFF force field cannot handle bond breaking. Did the authors sample the cluster structures using ionic monomers to simulate bond breaking (see Kubečka et al., https://doi.org/10.1021/acs.jpca.9b03853).

Only selecting the lowest 100 cluster configurations based on PM7 could lead to the global minimum cluster being missed (see Kurfman et al., https://doi.org/10.1021/acs.jpca.1c00872). Could the authors comment on this aspect?

Response: We thank Dr. Jonas Elm for these professional comments and apologize for the previously incomplete description of the configurational sampling. We have addressed the points as follows.

(i) We have moved the multi-step conformational search method from the SI into Section 2.1 of the revised manuscript, describing the full workflow: ABCluster generation → semi-empirical PM7 pre-screening → ωB97X-D/6-311++G(3df,3pd) optimization and frequency analysis → high-level DLPNO-CCSD(T) single-point correction.

(ii) Because the UFF force field cannot describe proton transfer, we utilized ion monomers for sampling during the cluster configuration search and had manually constructed some potential stable clusters with multiple hydrogen/halogen bonding sites based on chemical intuition. The relevant statements have been added in lines 81-84 and 87-88 of the revised manuscript as follows:

"Given the inability of the Universal Force Field (UFF) to describe proton transfer, ions in distinct protonation states were utilized to model hydrogen bonding and proton transfer. The ionic species considered include IO_3^-, NO_3^- and the protonated counterpart $H_2IO_2^+$."

"In addition, we manually constructed a set of candidate structures with multiple hydrogen- and halogen-bonding structures based on chemical intuition."

(iii) We acknowledge the limitation noted by Dr. Jonas Elm. Considering the computational cost, we retained 1000 local minima from each ABCluster search and carried forward the lowest 100 configurations based on PM7 single-point energies. As pointed out by Kurfman et al. (2021), this truncation may lead to the global minimum being missed. We have added the following statements into Section 2.1, lines 85–87, of the revised manuscript:

"Despite exhaustive sampling within the computational budget, selecting the lowest 100 configurations based on PM7 calculations may still result in the true global minimum being missed (Kurfman et al., 2021)."

Comment 2 (Line 74). *"All identified low-energy cluster conformations were rigorously optimized and subjected to frequency analysis using the Gaussian 09 package (Frisch et al., 2009) at the ωB97X-D/6-311++G(3df,3pd) (for H, O, N) + aug-cc-pVTZ-PP with ECP28MDF (for I) level of theory"*

I am missing some justification to why the ωB97X-D functional and why the 6-311++G(3df,3pd) basis set was used. There exist many benchmarks that advocate this level of theory, but without a proper reference it may seem like an arbitrary choice.

Response: We thank Dr. Jonas Elm for this constructive comment. We have added the supporting references in Section 2.2 of the revised manuscript. The ωB97X-D functional (Elm et al., 2013) together with the 6-311++G(3df,3pd) (Elm et al., 2012) basis set has been benchmarked and widely adopted for the noncovalent interactions of atmospheric molecular clusters, as it provides highly reliable estimates of binding energies.

Accordingly, we have added a sentence to explain our choice in lines 90-91 and 94-97 of the revised manuscript as follows:

"All subsequent Density Functional Theory (DFT) optimizations were performed with the Gaussian 09 package, consistently using the ωB97X-D functional and a FineGrid for integration, which has been benchmarked and widely adopted for describing noncovalent interactions in atmospheric molecular clusters (Elm et al., 2013)."

"To ensure accuracy for atmospheric systems, the 6-311++G(3df,3pd) basis set was assigned to H, O, and

N, in combination with the aug-cc-pVTZ-PP basis set and ECP28MDF for I (Francl et al., 1982; Peterson et al., 2003). As demonstrated by previous benchmark studies, this combination provides highly reliable estimates of binding energies (Elm et al., 2012, 2013)."

Comment 3 (Line 80, Eq. 1). I am missing some specification on how the spin-orbit coupling SOC was calculated. Could the authors please elaborate.

In addition, I believe it was Khanniche et al. (10.1016/j.comptc.2016.09.010, https://doi.org/10.1021/acsearthspacechem.6b00010) and Engsvang et al. (https://doi.org/10.1021/acsomega.4c01235) that suggested that SOC is important for iodine species in the atmosphere. It might be worth to explicitly acknowledging the previous foundational work in the manuscript.

Response: We thank Dr. Jonas Elm for highlighting these foundational studies. As pointed out, relativistic effects are highly pronounced in systems containing heavier atoms like iodine. The foundational work establishing the importance of spin-orbit coupling (SOC) for atmospheric iodine species has been formally cited in the revised manuscript (Khanniche et al., 2016, 2017; Engsvang et al., 2024).

In this study, the spin-orbit coupling energy correction (ΔE_{SOC}) for iodine-containing clusters was obtained using Gaussian 16 as the energy difference between two single-point calculations at the 6-311++G(3df,3pd) (for H, O and N) + dhfTZVP-2c (for I): (i) a Spin-orbit DFT (SODFT) framework, which includes both the scalar potential and spin-orbit orbital potentials; and (ii) a DFT calculation using the same basis set but without spin-orbit potential. ΔE_{SOC} is calculated as the difference E(SODFT) − E(DFT). We have elaborated the SOC treatment in Section 2.2, lines 106–111, of the revised manuscript as below:

"Spin-orbit coupling (SOC) effects play a significant role in the thermodynamic properties of atmospheric iodine species due to their heavy-atom nature, as previously demonstrated by foundational studies (Khanniche et al., 2016, 2017; Engsvang et al., 2024). In this study, the SOC correction (ΔE_{SOC}) was evaluated by computing the energy difference between calculations performed with and without SOC potential. These calculations were performed using Gaussian 16 (Frisch et al., 2016) at the ωB97X-D/6-311++G(3df,3pd) (for H, N and O) + dhfTZVP-2c (for I) level of theory (Chan and Yim, 2013; Kühn and Weigend, 2015; Sarr et al., 2021; Holzer et al., 2022)"

Comment 4 (Line 83). *"… DLPNO-CCSD(T)/aug-cc-pVTZ (for H, O, and N) + aug-cc-pVTZ-PP with ECP28MDF (for I) level of theory with TightPNO and TightSCF settings."*

Engsvang et al. (https://doi.org/10.1021/acsomega.4c01235) demonstrated that relativistic effects are important to include in the Hamiltonian. Even a simple scalar relativistic method such as ZORA was found to lead to a difference. Without relativistic correction the calculated binding energies likely lead to too stable clusters. The authors should comment on this aspect.

Response: We are highly grateful to Dr. Jonas Elm for raising this crucial point regarding the relativistic effects. Based on the approach of Engsvang et al. (2024), we performed additional single-point calculations using the zeroth-order regular approximation (ZORA) employing the ORCA program. For these calculations we used the ma-ZORA-def2-TZVPP basis set for H, N, and O atoms, and the SARC-ZORA-TZVPP basis set to describe I. The ZORA-corrected cluster Gibbs free energies (ΔG_{263}) at 263 K of all

optimized clusters are now reported in Table 1 below.

As shown in Table 1, ΔG_{263} obtained after ZORA correction are less negative (i.e., less stable) than the original DLPNO-CCSD(T) values, with the energy difference reaching up to ~20 kcal mol^{-1} for some of the six-molecule clusters. Using these energies, we simulated the binary HIO_3–HIO_2 cluster formation rates (J) under CLOUD chamber conditions. As shown in Figure 1, these newly obtained ZORA-corrected results (red line) were then compared with (a) the CLOUD experimental data (circles) and (b) our original DLPNO-CCSD(T) calculations (blue line). Consistent with the change in the binding energies, the J after ZORA correction is reduced substantially, whereas the original DLPNO-CCSD(T) method demonstrates closer agreement with the CLOUD experimental results.

We have placed the ZORA-corrected ΔG_{263} and the corresponding cluster formation rates in the revised Supplementary Information (Table S6 and Figure S11, respectively) to facilitate future methodological improvements and model intercomparison. However, considering that the J simulated by the original DLPNO-CCSD(T)/aug-cc-pVTZ (for H, O, N) + aug-cc-pVTZ-PP/ECP28MDF (I) method is in better agreement with the experimental results, we have retained this approach for the single-point correction.

Correspondingly, we have included a discussion regarding the ZORA-DLPNO-CCSD(T) calculations in the Uncertainty Analysis section, lines 404–412 of the revised manuscript:

"It is also worth noting the potential uncertainties related to the relativistic effects. A recent benchmark (Engsvang et al., 2024) has demonstrated that the ZORA-DLPNO-CCSD(T) approach, which incorporates the zeroth-order regular approximation (ZORA) (Lenthe et al., 1993) provides thermodynamic estimates that are highly consistent with reference ZORA-CCSD(T) calculations. To address this, we performed single-point energy calculations at the ZORA-DLPNO-CCSD(T)/ma-ZORA-def2-TZVPP (for H, N, and O) (Neese, 2012) + SARC-ZORA-TZVPP (for I) (Rolfes et al., 2020) level of theory using the ORCA program. To provide more precise thermodynamic energies, the ZORA-corrected results are listed in Table S6, and the subsequently simulated J are presented in Figure S11. Although it includes more comprehensive physical corrections, the ZORA-corrected energies tend to yield lower J values than the CLOUD measurements. Given that DLPNO-CCSD(T) method demonstrates closer agreement, we have retained it for single-point correction."

Table 1. Gibbs free energies (ΔG) evaluated at 263 K (kcal mol^{-1}) of the $(HNO_3)_x(HIO_3)_y(HIO_2)_z$ clusters ($2 \le x + y + z \le 6$, $0 \le x \le 3$). DLPNO-CCSD(T) values were computed at the DLPNO-CCSD(T)/aug-cc-pVTZ (for H, N, O) + aug-cc-pVTZ-PP with ECP28MDF (for I) level of theory; ZORA-DLPNO-CCSD(T) values were computed at the ZORA-DLPNO-CCSD(T)/ma-ZORA-def2-TZVPP (for H, N and O) + SARC-ZORA-TZVPP (for I) level of theory, both based on geometries optimized at the ωB97X-D/6-311++G(3df,3pd) + aug-cc-pVTZ-PP level.

Clusters	ΔG_{263K} (kcal mol^{-1})	
	DLPNO-CCSD(T)	ZORA-DLPNO-CCSD(T)
$(HIO_2)_2$	-19.9	-16.0
$(HIO_2)_3$	-37.7	-30.3
$(HIO_2)_4$	-54.7	-44.4
$(HIO_2)_5$	-69.3	-54.8
$(HIO_2)_6$	-87.3	-69.3
$(HIO_3)_1(HIO_2)_1$	-18.8	-15.7

$(HIO_3)_1(HIO_2)_2$	-38.7	-32.8
$(HIO_3)_1(HIO_2)_3$	-54.6	-43.1
$(HIO_3)_1(HIO_2)_4$	-73.0	-58.5
$(HIO_3)_1(HIO_2)_5$	-76.1	-57.3
$(HIO_3)_2$	-12.8	-8.7
$(HIO_3)_2(HIO_2)_1$	-35.6	-26.8
$(HIO_3)_2(HIO_2)_2$	-54.5	-44.4
$(HIO_3)_2(HIO_2)_3$	-74.7	-60.1
$(HIO_3)_2(HIO_2)_4$	-94.0	-74.9
$(HIO_3)_3$	-25.0	-16.4
$(HIO_3)_3(HIO_2)_1$	-49.0	-39.0
$(HIO_3)_3(HIO_2)_2$	-73.7	-58.4
$(HIO_3)_3(HIO_2)_3$	-98.8	-77.7
$(HIO_3)_4$	-44.1	-31.6
$(HIO_3)_4(HIO_2)_1$	-66.9	-48.8
$(HIO_3)_4(HIO_2)_2$	-90.7	-68.9
$(HIO_3)_5$	-60.5	-42.3
$(HIO_3)_5(HIO_2)_1$	-83.5	-61.8
$(HIO_3)_6$	-74.0	-50.3
$(HNO_3)_1(HIO_2)_1$	-13.0	-10.0
$(HNO_3)_1(HIO_2)_2$	-26.3	-19.9
$(HNO_3)_1(HIO_2)_3$	-46.7	-37.2
$(HNO_3)_1(HIO_2)_4$	-62.9	-51.2
$(HNO_3)_1(HIO_2)_5$	-80.1	-64.0
$(HNO_3)_1(HIO_3)_1$	-5.3	-3.8
$(HNO_3)_1(HIO_3)_1(HIO_2)_1$	-24.6	-18.7
$(HNO_3)_1(HIO_3)_1(HIO_2)_2$	-47.3	-37.0
$(HNO_3)_1(HIO_3)_1(HIO_2)_3$	-63.8	-48.9
$(HNO_3)_1(HIO_3)_1(HIO_2)_4$	-81.6	-63.5
$(HNO_3)_1(HIO_3)_2$	-18.1	-11.2
$(HNO_3)_1(HIO_3)_2(HIO_2)_1$	-41.2	-30.7
$(HNO_3)_1(HIO_3)_2(HIO_2)_2$	-60.0	-44.8
$(HNO_3)_1(HIO_3)_2(HIO_2)_3$	-89.2	-69.2
$(HNO_3)_1(HIO_3)_3$	-32.0	-20.8
$(HNO_3)_1(HIO_3)_3(HIO_2)_1$	-55.4	-39.2
$(HNO_3)_1(HIO_3)_3(HIO_2)_2$	-81.0	-59.7
$(HNO_3)_1(HIO_3)_4$	-49.8	-31.7
$(HNO_3)_1(HIO_3)_4(HIO_2)_1$	-75.7	-55.1
$(HNO_3)_1(HIO_3)_5$	-68.1	-47.7
$(HNO_3)_2$	-0.3	1.1
$(HNO_3)_2(HIO_2)_1$	-14.8	-11.2
$(HNO_3)_2(HIO_2)_2$	-40.0	-31.4
$(HNO_3)_2(HIO_2)_3$	-55.0	-43.7
$(HNO_3)_2(HIO_2)_4$	-74.5	-58.6
$(HNO_3)_2(HIO_3)_1$	-10.3	-6.3
$(HNO_3)_2(HIO_3)_1(HIO_2)_1$	-29.7	-21.6

$(HNO_3)_2(HIO_3)_1(HIO_2)_2$	-52.4	-40.6
$(HNO_3)_2(HIO_3)_1(HIO_2)_3$	-77.7	-60.5
$(HNO_3)_2(HIO_3)_2$	-25.7	-16.4
$(HNO_3)_2(HIO_3)_2(HIO_2)_1$	-46.7	-34.0
$(HNO_3)_2(HIO_3)_2(HIO_2)_2$	-62.4	-47.9
$(HNO_3)_2(HIO_3)_3$	-37.8	-25.1
$(HNO_3)_2(HIO_3)_3(HIO_2)_1$	-61.7	-43.7
$(HNO_3)_2(HIO_3)_4$	-53.0	-36.8
$(HNO_3)_3$	2.9	4.5
$(HNO_3)_3(HIO_2)_1$	-15.1	-9.2
$(HNO_3)_3(HIO_2)_2$	-37.8	-27.3
$(HNO_3)_3(HIO_2)_3$	-59.9	-46.6
$(HNO_3)_3(HIO_3)_1$	-14.1	-7.9
$(HNO_3)_3(HIO_3)_1(HIO_2)_1$	-33.0	-24.2
$(HNO_3)_3(HIO_3)_1(HIO_2)_2$	-56.0	-41.7
$(HNO_3)_3(HIO_3)_2$	-27.0	-16.4
$(HNO_3)_3(HIO_3)_2(HIO_2)_1$	-48.7	-34.6
$(HNO_3)_3(HIO_3)_3$	-42.6	-28.3

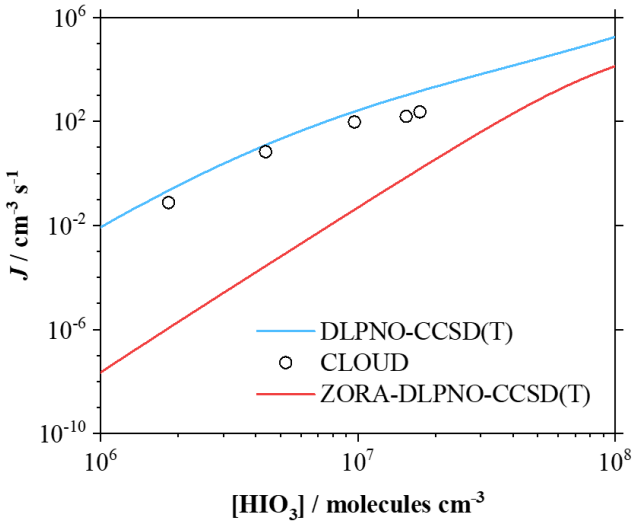

Figure 1. Cluster formation rates (J, cm^{-3} s^{-1}) of the HIO_3–HIO_2 system. Experimental data from the CLOUD chamber (He et al., 2021) are represented by circles. Theoretical ACDC simulations were evaluated at the DLPNO-CCSD(T)/aug-cc-pVTZ (for H, N, O) + aug-cc-pVTZ-PP with ECP28MDF (for I) level (blue line), and the ZORA-DLPNO-CCSD(T)/ma-ZORA-def2-TZVPP (for H, N, O) + SARC-ZORA-TZVPP (for I) level (red line). Simulations were performed under the same conditions as the CLOUD experiment: $[HIO_3] = 10^6$–10^8, $[HIO_2] = 2 \times 10^4$–2×10^6 molecules cm^{-3}, $T = 263$ K, and CS = 2.2×10^{-3} s^{-1}.

Comment 5 (Lines 108–111). Please mention the explicit boundary conditions in the main text. Setting the

boundary clusters as clusters consisting of only six molecules could lead to artefacts in the ACDC simulations, giving too high cluster formation rates (see Besel et al., https://doi.org/10.1021/acs.jpca.0c03984). Too small boundary cluster will yield too high cluster formation rates. This aspect should be elaborated in the manuscript.

Response: We thank Dr. Jonas Elm for the professional comment. The previously unclear description of the boundary conditions has been rectified. The specific boundary conditions are listed in Table S3 of the revised SI. To clarify, the simulation system encompasses clusters containing up to six molecules. The boundary conditions are seven-molecule clusters formed through the collision of a kinetically stable six-molecule cluster with one additional monomer (HNO_3, HIO_3, or HIO_2). The identity of these boundary conditions was determined individually at each simulation temperature using the $\beta c/\sum\gamma > 1$ criterion.

We have added the corresponding explanation in Section 2.4, lines 133–135, of the revised manuscript as below:

"Correspondingly, the boundary conditions are set as seven-molecule clusters, representing the smallest kinetically stable clusters that grow beyond the six-molecule simulation system."

We further acknowledge the referee's concern that, as demonstrated by Besel et al. (2020), small boundary clusters may overestimate the absolute cluster formation rate J. This effect may contribute to the modest exceedance of the field-observed upper limit discussed in our response to Comment 12.

Comment 6 (Section 3.1 and Figure 1). I do not see what Figure 1 is contributing with to the present study. It is simple chemistry to identify the donor/acceptor groups in molecules. No need for electrostatic potential maps for doing this. Please remove this part.

Instead it would be much more informative to include some of the cluster structures which are hidden in the SI.

Response: We thank Dr. Jonas Elm for this valuable suggestion. Following the referee's advice, we have moved the ESP analysis to Figure S1, and replaced it in the main text with a new Figure 1 showing representative optimized cluster structures. The new figure highlights the hydrogen bonds and halogen bonds that stabilize the $(HNO_3)_x(HIO_3)_y(HIO_2)_z$ clusters, providing a more direct chemical picture of cluster stabilization.

Comment 7 (Line 152). *"Six-molecule clusters with an acid-to-base ratio of 1:1 (HNO_3 and HIO_3 as acids, HIO_2 as base) exhibit the lowest Gibbs free energies of formation (ΔG). This 1:1 stoichiometry preference is consistent across all cluster sizes (Figure S2)."*

The 1:1 acid-to-base ratio is general finding in cluster formation studies. This was originally found by Olenius et al. (https://doi.org/10.1063/1.4819024) and generalized by Elm et al. (https://doi.org/10.1021/acs.jpca.7b08962). This finding should be put into context with previous work, as it is not a unique finding discovered here.

Response: We fully agree and apologize for not properly acknowledging the prior literature. Our work is an extension of this established finding to the HNO_3-iodine-oxoacid system. We have revised the relevant sentence, lines 180–182, to put this finding into context with previous work:

"Consistent with established thermodynamic patterns in acid-base clustering (Olenius et al., 2013; Elm, 2017), six-molecule clusters with an acid-to-base ratio of 1:1 (HNO_3 and HIO_3 as acids, HIO_2 as base) exhibit the lowest Gibbs free energies of formation (ΔG)."

Comment 8 (Line 165). *"Although HNO_3-containing clusters require a higher cboundary than HIO_3–HIO_2 clusters, ambient HNO_3 concentrations (10^8–10^{11} molecules/cm^3), spanning clean polar regions to polluted coastal environments"*

Could you add a reference here for HNO_3 reaching 10^8 molecules cm^{-3} in clean polar regions?

Response: Thanks for the valuable suggestions. The HNO_3 concentrations of ~10^8 molecules cm^{-3} in clean polar air correspond to the measurements at Summit, Greenland (Honrath et al., 2002), as well as the Antarctic HNO_3 observations (Jones et al., 2014). To make the data sources clearer, we have explicitly added these two references corresponding to polar regions in Section 3.3, lines 216–219, of the revised manuscript:

"HNO_3 concentrations were set to 10^8–10^{11} molecules cm^{-3} (from remote polar regions (Honrath et al., 2002; Jones et al., 2014) to polluted coastal areas (Xu et al., 2018)) …"

Comment 9 (Line 174). I do not understand Figure 2(b). How can clusters that do not include HNO_3 depend on its concentration for $c_{boundary}$?

Response: We thank Dr. Jonas Elm for pointing out this inconsistency, and apologize for the confusion. We fully agree that the $c_{boundary}$ of pure HIO_3–HIO_2 clusters is independent of the HNO_3 concentration, as they do not contain HNO_3. Consequently, to prevent misleading interpretations, we have removed the pure iodine oxoacid clusters from the revised Figure 2(b). We have also refined Figure S4 by excluding the irrelevant $c_{boundary}$ thresholds for absent species, such as HIO_3 collisions involving non-HIO_3-containing clusters.

Comment 10 (Line 206). *"Given the ppb-level HNO_3 concentrations observed in the UT, this enhanced sensitivity underscores the amplified importance of HNO_3 in iodine oxoacid nucleation at high altitudes."*

Do you have a reference for HNO_3 reaching 1 ppb in the UT?

Response: Yes. The sub-ppb to ppb levels of HNO_3 concentration in the UT and tropopause regions are supported by the aircraft measurements of Jurkat et al. Specifically, their study explicitly reported that HNO_3 concentrations can exceed 1 ppb in the UT. We have cited for the precursor profiles in Section 3.4, lines 247-248:
"matching the concentration distributions of the nucleation precursors at different altitudes in the atmosphere (Jurkat et al., 2014)."

Comment 11 (Line 223). *"HIO_3 concentration was set to 1×10^7 molecules cm^{-3} in the MBL (coastal emission hotspot) (Sipilä et al., 2016) and reduced by one order of magnitude in the FT. Due to limited field constraints on HIO3 at high altitudes, its concentration was held constant above the FT."*

I am a bit concerned that the iodine oxoacid concentrations might be a bit too high in the UT. Has it actually been proven that iodine oxoacids can be transported to the upper troposphere or just been inferred? From the cited work (Twohy et al., 2002; Randel et al., 2010; Williamson et al., 2019), I only find mention of convective clouds, but not that they can transport iodine. Would iodine species formed in the lower troposphere not quite rapidly form particles and thereby be scavenged before being transported to the upper troposphere?

Response: This is an important and thoughtful concern. We acknowledge that the originally cited convective-transport references (Twohy et al., 2002; Randel et al., 2010; Williamson et al., 2019) were intended to illustrate the general physical connection between the lower and upper troposphere, and indeed did not directly address iodine concentrations at altitude. Nevertheless, iodine has been directly observed at high altitude: quantitative particulate iodine has been detected in the upper troposphere (Koenig et al., 2020), and HIO_3 along with molecular clusters have been directly measured in the marine free troposphere (Salignat et al., 2024). Given the scarcity of direct measurements of iodine oxoacids at high altitudes, the UT iodine oxoacid concentrations used in our simulations are inferred, primarily because in-situ chemical production at altitude is likely to play a significant role. Since HIO_3 can form in-situ from the IO radical (Finkenzeller et al., 2023), which exhibits a relatively altitude-invariant profile (Koenig et al., 2020), high-altitude HIO_3 can be sustained by local oxidation of IO without requiring intact uplift of HIO_3 itself. The statement in lines 254-259 of the revised manuscript is as follows:

"Due to limited field constraints on HIO_3 at high altitudes, its concentration was held constant above the FT. This assumption is based on the fact that the concentration of iodine monoxide (IO) radical, a key precursor of HIO_3 in the troposphere with relatively stable concentrations across altitudes (Koenig et al., 2020), exhibits an observed positive correlation with that of HIO_3 in the troposphere (Finkenzeller et al., 2023). HIO_2 concentration was fixed at a ratio of 1/50 relative to HIO_3 across all altitudes, consistent with the conditions in Figure 3."

Given the limited field constraints on UT iodine concentrations, we additionally performed sensitivity analyses on [HIO_3] and [HIO_2] (Figs. S7 and S8). These analyses confirm that the altitude-dependent role transition of HNO_3 from an MBL catalyst to a UT core component holds across a wide range of iodine oxoacid concentrations, including substantially lower UT values than those used in the base-case simulation. We thank the referee for this insightful comment.

Comment 12 (Line 315). *"Both HNO_3-HIO_3-HIO_2 and HIO_3-HIO_2 mechanisms are consistent with the upper limit of field-observed cluster formation rates."*

In figure 6(a) and 6(b) it is seen that both mechanisms actually exceed the observed upper limit. I suspect this could be related to too strongly binding clusters. As mentioned under methods above this could originate either from the boundary conditions or the applied quantum chemical methods. This aspect should be further commented on.

Response: We agree with Dr. Jonas Elm and have revised the wording. Instead of "consistent with the upper limit", the revised sentence now states that both mechanisms reach or modestly exceed the observed upper limit of the field-reported cluster formation rates. This modest exceedance most likely reflects two factors:

(i) Boundary-cluster size. As noted in our response to Comment 5, considering that nitric acid clusters may

exhibit relatively high evaporation rates at higher temperatures, a seven-molecule boundary might not reach the critical cluster size, potentially leading to an overestimation of the absolute *J* (Besel et al., 2020).

(ii) Possible overbinding of the quantum chemical method, as suggested by a previous benchmark (Engsvang et al., 2024).

Accordingly, we have incorporated the discussion of these two potential factors into the analysis in Section 3.5, lines 346–350, of the revised manuscript:

"Both the HNO_3–HIO_3–HIO_2 and HIO_3–HIO_2 mechanisms generally reach, and at higher concentrations modestly exceed, the upper limit of field-observed cluster formation rates. This potential overestimation of *J* likely originates from methodological limitations: specifically, the finite seven-molecule boundary may not encompass the critical cluster size (Besel et al., 2020), and the applied quantum chemical level of theory might inherently produce slightly overbound clusters (Engsvang et al., 2024)."

Comment 13 (Line 344). I commend the authors for making a section on the potential uncertainties in the quantum chemical results and applied concentration. However, based on previous benchmarks, it should be explicitly stated that it is more likely that the applied methods are yielding too low free energies. Hence, the +1 kcal/mol scenario is probably the most likely.

Response: We thank Dr. Jonas Elm for this valuable suggestion. We have added a statement in Section 3.6, lines 391–393, of the revised manuscript:

"As indicated by prior benchmarks (Schmitz and Elm, 2020; Engsvang et al., 2024), the DLPNO-CCSD(T) method may slightly underestimate ΔG (i.e., over-bind the clusters). Therefore, the +1 kcal mol^{-1} perturbation is likely the most realistic scenario."

We are grateful to Dr. Jonas Elm for the detailed and expert comments, which have substantially improved the methodological transparency and robustness of the results. All revisions are highlighted in the revised manuscript and the Supporting Information.

Sincerely,

Xiuhui Zhang
Key Laboratory of Cluster Science, Ministry of Education of China
School of Chemistry and Chemical Engineering, Beijing Institute of Technology
Beijing 100081, P. R. China
Email: zhangxiuhui@bit.edu.cn

Reference:

Besel, V., Kubečka, J., Kurtén, T., and Vehkamäki, H.: Impact of Quantum Chemistry Parameter Choices and Cluster Distribution Model Settings on Modeled Atmospheric Particle Formation Rates, J. Phys. Chem. A, 124, 5931–5943, https://doi.org/10.1021/acs.jpca.0c03984, 2020.

Chan, B. and Yim, W.-L.: Accurate Computation of Cohesive Energies for Small to Medium-Sized Gold Clusters, J. Chem. Theory Comput., 9, 1964–1970, https://doi.org/10.1021/ct400047y, 2013.

Elm, J.: Elucidating the Limiting Steps in Sulfuric Acid–Base New Particle Formation, J. Phys. Chem. A,

121, 8288–8295, https://doi.org/10.1021/acs.jpca.7b08962, 2017.

Elm, J., Bilde, M., and Mikkelsen, K. V.: Assessment of Density Functional Theory in Predicting Structures and Free Energies of Reaction of Atmospheric Prenucleation Clusters, J. Chem. Theory Comput., 8, 2071–2077, https://doi.org/10.1021/ct300192p, 2012.

Elm, J., Bilde, M., and Mikkelsen, K. V.: Assessment of binding energies of atmospherically relevant clusters, Phys. Chem. Chem. Phys., 15, 16442, https://doi.org/10.1039/c3cp52616j, 2013.

Engsvang, M., Wu, H., and Elm, J.: Iodine Clusters in the Atmosphere I: Computational Benchmark and Dimer Formation of Oxyacids and Oxides, ACS Omega, 9, 31521–31532, https://doi.org/10.1021/acsomega.4c01235, 2024.

Finkenzeller, H., Iyer, S., He, X.-C., Simon, M., Koenig, T. K., Lee, C. F., Valiev, R., Hofbauer, V., Amorim, A., Baalbaki, R., Baccarini, A., Beck, L., Bell, D. M., Caudillo, L., Chen, D., Chiu, R., Chu, B., Dada, L., Duplissy, J., Heinritzi, M., Kemppainen, D., Kim, C., Krechmer, J., Kürten, A., Kvashnin, A., Lamkaddam, H., Lee, C. P., Lehtipalo, K., Li, Z., Makhmutov, V., Manninen, H. E., Marie, G., Marten, R., Mauldin, R. L., Mentler, B., Müller, T., Petäjä, T., Philippov, M., Ranjithkumar, A., Rörup, B., Shen, J., Stolzenburg, D., Tauber, C., Tham, Y. J., Tomé, A., Vazquez-Pufleau, M., Wagner, A. C., Wang, D. S., Wang, M., Wang, Y., Weber, S. K., Nie, W., Wu, Y., Xiao, M., Ye, Q., Zauner-Wieczorek, M., Hansel, A., Baltensperger, U., Brioude, J., Curtius, J., Donahue, N. M., Haddad, I. E., Flagan, R. C., Kulmala, M., Kirkby, J., Sipilä, M., Worsnop, D. R., Kurten, T., Rissanen, M., and Volkamer, R.: The gas-phase formation mechanism of iodic acid as an atmospheric aerosol source, Nat. Chem., 15, 129–135, https://doi.org/10.1038/s41557-022-01067-z, 2023.

Frisch, M. J., Trucks, G. W., Schlegel, H. B., Scuseria, G. E., Robb, M. A., Cheeseman, J. R., Scalmani, G., Barone, V., Mennucci, B., Petersson, G. A., Nakatsuji, H., Caricato, M., Li, X., Hratchian, H. P., Izmaylov, A. F., Bloino, J., Zheng, G., Sonnenberg, J. L., Hada, M., Ehara, M., Toyota, K., Fukuda, R., Hasegawa, J., Ishida, M., Nakajima, T., Honda, Y., Kitao, O., Nakai, H., Vreven, T., Montgomery, J. A., Peralta, J. E., Ogliaro, F., Bearpark, M., Heyd, J. J., Brothers, E., Kudin, K. N., Staroverov, V. N., Kobayashi, R., Normand, J., Raghavachari, K., Rendell, A., Burant, J. C., Iyengar, S. S., Tomasi, J., Cossi, M., Rega, N., Millam, J. M., Klene, M., Knox, J. E., Cross, J. B., Bakken, V., Adamo, C., Jaramillo, J., Gomperts, R., Stratmann, R. E., Yazyev, O., Austin, A. J., Cammi, R., Pomelli, C., Ochterski, J. W., Martin, R. L., Morokuma, K., Zakrzewski, V. G., Voth, G. A., Salvador, P., Dannenberg, J. J., Dapprich, S., Daniels, A. D., Farkas, O., Foresman, J. B., Ortiz, J. V., Cioslowski, J., and Fox, D. J.: Gaussian 16, Revision A.03; Gaussian, Inc.: Wallingford CT, 2016.

Holzer, C., Franzke, Y. J., and Pausch, A.: Current density functional framework for spin–orbit coupling, J. Chem. Phys., 157, 204102, https://doi.org/10.1063/5.0122394, 2022.

Honrath, R. E., Lu, Y., Peterson, M. C., Dibb, J. E., Arsenault, M. A., Cullen, N. J., and Steffen, K.: Vertical fluxes of NO_x, HONO, and HNO_3 above the snowpack at Summit, Greenland, Atmos. Environ., 36, 2629–2640, https://doi.org/10.1016/S1352-2310(02)00132-2, 2002.

Jones, A. E., Brough, N., Anderson, P. S., and Wolff, E. W.: HO_2NO_2 and HNO_3 in the coastal Antarctic winter night: a “lab-in-the-field” experiment, Atmos. Chem. Phys., 14, 11843–11851, https://doi.org/10.5194/acp-14-11843-2014, 2014.

Jurkat, T., Voigt, C., Kaufmann, S., Zahn, A., Sprenger, M., Hoor, P., Bozem, H., Müller, S., Dörnbrack, A., Schlager, H., Bönisch, H., and Engel, A.: A quantitative analysis of stratospheric HCl, HNO_3, and O_3 in the tropopause region near the subtropical jet, Geophys. Res. Lett., 41, 3315–3321,

https://doi.org/10.1002/2013GL059159, 2014.

Khanniche, S., Louis, F., Cantrel, L., and Černušák, I.: A theoretical study of the microhydration of iodic acid ($HOIO_2$), Comput. Theor. Chem., 1094, 98–107, https://doi.org/10.1016/j.comptc.2016.09.010, 2016.

Khanniche, S., Louis, F., Cantrel, L., and Černušák, I.: Thermochemistry of HIO_2 Species and Reactivity of Iodous Acid with OH Radical: A Computational Study, ACS Earth Space Chem., 1, 39–49, https://doi.org/10.1021/acsearthspacechem.6b00010, 2017.

Koenig, T. K., Baidar, S., Campuzano-Jost, P., Cuevas, C. A., Dix, B., Fernandez, R. P., Guo, H., Hall, S. R., Kinnison, D., Nault, B. A., Ullmann, K., Jimenez, J. L., Saiz-Lopez, A., and Volkamer, R.: Quantitative detection of iodine in the stratosphere, Proc. Natl. Acad. Sci. U.S.A., 117, 1860–1866, https://doi.org/10.1073/pnas.1916828117, 2020.

Kühn, M. and Weigend, F.: Two-component hybrid time-dependent density functional theory within the Tamm-Dancoff approximation, J. Chem. Phys., 142, 034116, https://doi.org/10.1063/1.4905829, 2015.

Kurfman, L. A., Odbadrakh, T. T., and Shields, G. C.: Calculating Reliable Gibbs Free Energies for Formation of Gas-Phase Clusters that Are Critical for Atmospheric Chemistry: $(H_2SO_4)_3$, J. Phys. Chem. A, 125, 3169–3176, https://doi.org/10.1021/acs.jpca.1c00872, 2021.

Lenthe, E. V., Baerends, E. J., and Snijders, J. G.: Relativistic regular two-component Hamiltonians, The Journal of Chemical Physics, 99, 4597–4610, https://doi.org/10.1063/1.466059, 1993.

Neese, F.: The ORCA program system, WIREs Computational Molecular Science, 2, 73–78, https://doi.org/10.1002/wcms.81, 2012.

Olenius, T., Kupiainen-Määttä, O., Ortega, I. K., Kurtén, T., and Vehkamäki, H.: Free energy barrier in the growth of sulfuric acid–ammonia and sulfuric acid–dimethylamine clusters, J. Chem. Phys., 139, 084312, https://doi.org/10.1063/1.4819024, 2013.

Rolfes, J. D., Neese, F., and Pantazis, D. A.: All-electron scalar relativistic basis sets for the elements Rb–Xe, J. Comput. Chem., 41, 1842–1849, https://doi.org/10.1002/jcc.26355, 2020.

Salignat, R., Rissanen, M., Iyer, S., Baray, J.-L., Tulet, P., Metzger, J.-M., Brioude, J., Sellegri, K., and Rose, C.: Measurement report: Insights into the chemical composition and origin of molecular clusters and potential precursor molecules present in the free troposphere over the southern Indian Ocean: observations from the Maïdo Observatory (2150 m a.s.l., Réunion), Atmos. Chem. Phys., 24, 3785–3812, https://doi.org/10.5194/acp-24-3785-2024, 2024.

Sarr, S., Graton, J., Rahali, S., Montavon, G., and Galland, N.: Delocalized relativistic effects, from the viewpoint of halogen bonding, Phys. Chem. Chem. Phys., 23, 4064–4074, https://doi.org/10.1039/D0CP05840H, 2021.

Schmitz, G. and Elm, J.: Assessment of the DLPNO Binding Energies of Strongly Noncovalent Bonded Atmospheric Molecular Clusters, ACS Omega, 5, 7601–7612, https://doi.org/10.1021/acsomega.0c00436, 2020.

Xu, W., Liu, L., Cheng, M., Zhao, Y., Zhang, L., Pan, Y., Zhang, X., Gu, B., Li, Y., Zhang, X., Shen, J., Lu, L., Luo, X., Zhao, Y., Feng, Z., Collett Jr., J. L., Zhang, F., and Liu, X.: Spatial–temporal patterns of inorganic nitrogen air concentrations and deposition in eastern China, Atmos. Chem. Phys., 18, 10931–

10954, https://doi.org/10.5194/acp-18-10931-2018, 2018.